

The Role of Breaking Wavelets in Air-Sea Gas Transfer

G. T. CSANADY

Department of Oceanography, Old Dominion University, Norfolk, Virginia

Molecular diffusion sustains the flux of soluble gases on the water side of the air-sea interface. The "handover" of this flux to more efficient eddy mixing begins with the smallest eddies, of size l , which interact with the surface diffusion boundary layer (DBL), of thickness δ . Owing to the discrepancy of the scales, $\delta \ll l$, the flow field on the δ scale consists of horizontal motions of a velocity constant with depth and varying horizontally on the l scale. The vertical velocity is proportional to the divergence of the horizontal flow and increases linearly with depth. An exact solution of the advection-diffusion equation for the simple model of divergent stagnation point flow shows the mass transfer coefficient (velocity) k to be proportional to $(aD)^{1/2}$ and DBL thickness δ to be proportional to $(D/a)^{1/2}$, where a is divergence, D diffusivity. Over a solid wall a similar model of Hiemenz flow yields a more complex relationship, also involving viscosity. These models reveal the mechanism by which the DBL is kept thin. The most intense surface divergences on a wind-blown sea surface are associated with rollers on breaking wavelets. Vorticity and divergence in the rollers are both proportional to u^{*2}/ν , where u^* is friction velocity and ν is viscosity. The mass transfer coefficient resulting from divergences of this magnitude is then given by $k = \text{const } u^* Sc^{-1/2}$, where Sc is Schmidt number. Exact solutions of the advection-diffusion equation for model rollers reveal the details of the handover process. A thin DBL is maintained over divergences by the upward velocity. At convergences, narrow downward plumes convey DBL fluid into the turbulent interior. Flux lines (analogous to streamlines) are horizontal over divergences and dive down under convergences. Application to the sea surface requires a parameter quantifying the surface density of divergences. Laboratory data imply that a substantial fraction of the surface is covered by the divergences at higher wind speeds. However, in the open ocean straining by the large waves, and especially whitecapping, may significantly reduce the density of divergences and with it the area-average gas transfer rate. On the other hand, bubble and droplet production in whitecaps may diminish this effect or even reverse it.

1. INTRODUCTION

The exchange of gases between the ocean and the atmosphere is important in various global balances, notably in the carbon cycle, influenced by ocean storage of carbon dioxide. Henry's law determines the surface concentration of gases similar in behavior to CO_2 , and the exchange is driven by the concentration difference from surface to mixed layer interior. On account of low gas diffusivity in water, resistance to mass transfer in the air is negligible in comparison with that in water [Bolin 1960]. The resistance resides in a "diffusion boundary layer" (DBL), of which the thickness δ may be calculated from standard formulae and observed gas transfer rates to be of the order of $10 \mu\text{m}$. The detailed mechanism of air-sea gas transfer remains, however, obscure.

In the last decade or so, a number of thorough and imaginative investigations on the mechanism of gas to liquid mass transfer have been carried out in laboratory flumes. Their results have recently been summarized by Jähne *et al.* [1987]. Some key findings are as follows:

1. Above an air speed of about 5 m s^{-1} the gas transfer rate increases rapidly, in parallel with the increase of mean square total wave slope. (The slope of capillary waves behaves differently).

2. In the same speed range the mass transfer coefficient varies with the inverse square root of the Schmidt number (there is no separate Reynolds number dependence).

Earlier, Hasse and Liss [1980, p. 478] reviewed air-sea gas transfer and concluded that "The rather spectacular increase of gas exchange observed in wind tunnels with the onset of capillary waves has yet to receive a full explanation." In

view of the later results, one must interpret the appearance of capillaries as a symptom of other changes. Hasse and Liss then went on to discuss another major puzzle, the discrepancy between laboratory and field data on gas transfer.

The field data come mainly from radon evasion measurements [Broecker and Peng, 1974; Peng *et al.*, 1979], which show no increase of gas transfer rate with wind speed beyond about 10 m s^{-1} . Deacon [1981] attempted to reconcile the two data sets by filtering the field data on the basis of wind persistence. This is justified by the fact that the radon evasion method gives a several-day moving average of the gas transfer rate. Deacon concluded that the field data judged to originate from steady wind conditions, while subject to large scatter, do not conflict with the laboratory data up to 14 m s^{-1} wind speed. This may be true as far as it goes, but it does not explain some very low observed transfer rates in winds up to 19 m s^{-1} , steady or not. To reconcile those with observation, on the hypothesis that the laboratory data remain valid, one would have to suppose something to the effect that high present winds are correlated with dead calm past winds. Jähne *et al.* [1987] pointed out, however, that once the importance of waves to gas transfer is admitted, there is wide scope for the variation of field gas transfer with wave climate. They did not discuss how precisely this may come about.

Before attempting to explain wave effects on gas transfer, it is helpful to examine what the flow field is like on the microscopic scale δ of the DBL. This layer is much thinner than the smallest eddy or the shortest wave, so that the surface appears on this scale as a smooth flat plane (except around droplets or bubbles with diameters of the order of δ). Horizontal motions within the surface are possible. However, variations of horizontal velocity occur on a much

Copyright 1990 by the American Geophysical Union.

Paper number 89JC02787.
0148-0227/90/89JC-02787\$05.00

longer scale than δ , so that the velocity components u , v are very nearly constant with depth in the DBL. The vertical velocity vanishes at the surface, and grows linearly with depth,

$$w = -z(\partial u/\partial x + \partial v/\partial y)$$

Where the horizontal flow is divergent, the vertical velocity is upward, so that the DBL is squeezed by advection. In a region of surface convergence, the vertical velocity is downward, and the DBL is pulled down. The discrepancy of the scales δ and l makes a simple analysis of the advection-diffusion problem possible, as was first demonstrated by *Fortescue and Pearson* [1967]. The analysis shows that if some fraction of the surface contains divergent flow, the squeezing of the DBL by the upward motion may well control the layer thickness δ .

The flow structure and other mechanical properties of laboratory flume wavelets were investigated in great detail at Tohoku University of Y. Toba and his collaborators [see *Toba*, 1985; *Ebuchi et al.*, 1987]. The waves studied were typically some 10 cm long and 1 cm high. One of the Tohoku studies, due to *Okuda* [1982], clearly identified flow separation (in a wave-following frame of reference) near the steeper wavelet crests, and the accumulation of vortical fluid in the "roller" (separated flow region). The proximate cause of the flow separation may have been a shear stress spike upwind of the wave crest, where the local shear stress was several times greater than the mean. The surface vorticity of the fluid under the shear stress spike was stress divided by viscosity (the stress magnitude was inferred from this relationship). The fluid in the roller had vorticity of the same order. Kinematics of the flow in the roller requires it to be divergent at the trailing stagnation point. Observation showed the divergence to be rather less than the roller vorticity but much higher than the divergence due to wave orbital motions.

The Tohoku University results suggest a possible explanation for the observed effect of waves on gas transfer: if rollers on breaking wavelets generate high surface divergence, they could be the principal means of maintaining a thin surface DBL. If roller divergence is proportional to the surface vorticity and therefore varies inversely with viscosity, a pure Schmidt number dependence should result. This scenario is investigated below by constructing a model roller and calculating the rate of gas transfer.

The results indeed show pure Schmidt number dependence, in accordance with observation. An empirical parameter expresses the surface density of rollers. The magnitude of this parameter, fitted to observation, turns out to be credible. More important, increasing density of rollers in higher winds explains the observed parallel increase of rms wave slope and gas transfer. In the open ocean the density of short-wave rollers should also depend on long-wave orbital motions, long-wave breaking, and whitecapping. The production of bubbles and spray in large breakers is further likely to influence gas transfer. A combination of such effects may explain the scatter of field gas transfer data and their divergence from laboratory results.

2. THE MECHANISM OF GAS EXCHANGE AT THE SEA SURFACE

The transfer of mass between a flowing gas and an underlying liquid, in which the gas is soluble but nonreac-

tive, has interested chemical engineers for a long time. They have recognized for more than half a century that the main resistance to mass transfer lies in a thin diffusion boundary layer at the top of the liquid, adjacent to the free surface. For an excellent review of ideas on this problem originating in the chemical engineering literature see *Brtko and Kabel* [1978]. *Bolin* [1960] pointed out that the air-sea transfer of gases such as CO_2 is similarly controlled by a DBL. *Deacon* [1977] has reviewed the problem from the point of view of turbulent boundary layer theory and developed a gas transfer model based on a postulated analogy of the flow under the free surface with turbulent shear flow over a solid wall. He showed that the wall-layer model gives accurate estimates of gas transfer at low wind speeds but seriously underpredicts transfer rates at wind speeds greater than about 5 m s^{-1} .

The wall layer analogy is imperfect because horizontal motions at a free surface are possible, while they are prevented by a solid wall. This has the consequence that the velocity normal to the free surface varies inversely with the distance from the surface, rather than with the distance squared, as over a solid wall. *Ledwell* [1984] has allowed for this property of free surface flow by setting the eddy flux proportional to the surface divergence of the eddying motions. Using further scaling arguments, he deduced from this the correct Schmidt number dependence of the mass transfer coefficient. However, in his detailed model the total flux is assumed to consist of a linear superposition of molecular and eddy flux, as in many other turbulent flow models. Eddy-resolving model calculations demonstrate that the idea of an eddy flux independent of molecular diffusion is wrong (see Figure 3 below). *Ledwell's* model is therefore grossly unrealistic at depths of a few DBL thicknesses. Nor does it come to grips with the question why wavelets should affect gas transfer.

In an attempt to throw some light on this question, *Coantic* [1986] discussed the interaction of turbulent shear flow at the free surface with capillary waves. *Coantic's* arguments are similar to *Ledwell's* and are subject to the same criticism. In any case, capillaries are not the principal agents of enhancing free surface gas transfer, as has been pointed out above.

The basic difficulty with conventional eddy flux models is the Reynolds analogy: if eddies alone maintain some flux near the surface, they should transport all properties, momentum, heat, and mass, at the same rate at a given depth, as they indeed do in the well-mixed interior of the "mixed" layer. The analogy, or the equivalent mixing length arguments, are valid if the distribution of the transported property is smooth on the eddy length scale. Otherwise the inherent nonlinearity of advection comes into play, making the "eddy" flux dependent on molecular diffusivity in a region of sharp property gradients, just below the DBL in the case of free surface fluxes.

An approach alternative to the eddy flux models again comes from chemical engineering, from early intuitive ideas on "penetration," due to *Higbie* [1935], and on "surface renewal" due to *Danckwerts* [1951]. *Higbie* postulated that eddies occupy the surface for short periods and pick up gas; *Danckwerts* postulated that they periodically renew the surface. *Higbie* represented the resulting gas transfer process by a penetration time θ_c , during which an eddy is charged with gas at the surface; *Danckwerts* represented it

by a surface renewal rate s , or reciprocal age of fluid elements occupying the surface.

While these ideas were illuminating, they shared the main weakness of the eddy flux models in that they glossed over the details of the important handover process from molecular diffusion at the surface to eddy transport below. Penetration time or surface renewal rate are no less arbitrary than eddy diffusivity: their dependence on molecular diffusivity is not taken into account; nor is any effect of wavelets. It is also unclear how to reconcile eddy exposure at the surface or surface renewal with the kinematics of a fluid continuum.

Fortescue and Pearson [1967] were the first correctly to identify the processes involved in the handover process. They analyzed advection and diffusion near the surface of a liquid in a regular field of cellular eddies. The implications of this work have not been fully assimilated into the oceanographic literature. The concentration field calculated by Fortescue and Pearson clearly shows a thin DBL over the ascending branch of the flow. The descending branch, on the other hand, carries the surface fluid downward in a plume, where the vertical gradients are small. The surface flux associated with this eddy field is readily inferred from surface gradients: high over the ascending flow, low over the descending plume. Concentration isopleths are horizontal over a large part of the ascending fluid. In this portion of the field the horizontal velocity is divergent. The average mass transfer coefficient was calculated by Fortescue and Pearson to be

$$k = 1.46(uD/L)^{1/2} \quad (1)$$

where u is eddy velocity amplitude, L is cell size, and D is diffusivity: uD/L is the product of diffusivity and typical surface divergence.

Fortescue and Pearson took the cell size to equal the length scale of the energy containing eddies in the turbulent flow below the surface, the velocity amplitude the rms turbulent velocity. *Lamont and Scott* [1970] pointed out that the surface divergences so estimated were too feeble to account for observed gas transfer rates, and they emphasized the importance of the smaller eddies. In either case, however, the divergences were attributed by these authors to eddies generated by the shear flow in the liquid. It is difficult to account in this manner for the high intensity of surface divergence necessary to make (1) fit the data. The observed influence of wavelets on gas transfer across the air-sea interface suggests instead that at wind speeds greater than 5 m s^{-1} , the important divergences on a wind-blown surface are wavelet related. *Deacon* [1981] has shown that the divergences due to orbital motions are not strong enough to explain wavelet effects on gas transfer. This then leads to the proposition that divergences generated by the rollers on breaking wavelets are responsible. That proposition is examined here in quantitative detail.

3. ADVECTION-DIFFUSION IN FREE-SURFACE STAGNATION POINT FLOW

As already mentioned, surface renewal or eddy exposure taken literally is incompatible with fluid kinematics. Unless the free surface is supposed to fold over in the manner of a "plunging" breaker, it remains composed of the same fluid particles. If one excludes folding-over as a process significant in gas transfer, on account of infrequent occurrence,

surface divergence remains the only means of bringing fluid from the interior to the proximity of the surface. In order to entrain the DBL, eddies must transport well-mixed fluid up close to the surface and allow it to dive down again, carrying excess or deficiency of concentration acquired in the DBL. In the region of surface divergence, vertical advection works against downward diffusion to keep the DBL thin and the surface flux high. One suspects therefore that a formula similar to (1) may apply to mass transfer in a less regular eddy field than envisaged in Fortescue and Pearson's simple model.

The essence of the divergence effect is indeed revealed by a model yet simpler than Fortescue and Pearson's: divergent two-dimensional stagnation point flow at a plane free surface (with slip allowed, the air being so much less massive than water). Viscous effects are in this problem negligible, and the flow in the neighborhood of a surface divergence line may be described by the stream function

$$\psi = axz \quad (2a)$$

The free surface is the $z = 0$ line, neglecting the small surface displacements associated with pressure variations in the fluid (much as in linearized surface wave theory). The velocity components in the xz plane are

$$u = ax \quad w = -az \quad (2b)$$

and $a > 0$ is the divergence of the horizontal velocity. The diffusion of a scalar property χ in such a flow field is subject to the conservation law:

$$u \frac{\partial \chi}{\partial x} + w \frac{\partial \chi}{\partial z} = D \nabla^2 \chi \quad (3)$$

where D is molecular diffusivity. One expects the upward motion along the stagnation streamline $x = 0$ to squeeze the χ field close to the surface. In view of the symmetry of the flow field about this line, $\partial \chi / \partial x$ vanishes here. Because there is no reason why sharp horizontal concentration gradients should arise, it may be postulated, subject to verification, that horizontal diffusion is negligible, $D \partial^2 \chi / \partial x^2 = 0$. The distribution of χ along the x axis should then be given by the solution of the ordinary differential equation

$$w \frac{d\chi}{dz} = D \frac{d^2 \chi}{dz^2} \quad (4)$$

It is convenient to solve first for the molecular flux F

$$F = -D \frac{d\chi}{dz} \quad (5)$$

which is subject to the equation

$$\frac{dF}{dz} = -\frac{azF}{D} \quad (6)$$

It is important to stipulate that the solution describes only the DBL, where molecular diffusion dominates. Outside this layer the concentration gradient and the molecular flux are vanishingly small. Correspondingly, the boundary conditions on (6) are

$$\begin{aligned} F &= F_0 & z &= 0 \\ F &= 0 & z &\rightarrow -\infty \end{aligned} \quad (7)$$

with the magnitude of F_0 remaining to be determined. The solution is:

$$F = F_0 \exp\left(-\frac{az^2}{2D}\right) \quad (8)$$

The concentration distribution is now found by integration. Of interest is the concentration excess or deficit in the DBL. Putting therefore $\chi(-\infty) = 0$,

$$\chi = -\frac{F_0}{D} \int_{-\infty}^z \exp\left(-\frac{az^2}{2D}\right) dz = \chi_0 \operatorname{erfc}\left[z\left(\frac{a}{2D}\right)^{1/2}\right] \quad (9a)$$

where

$$\chi_0 = -F_0 \left(\frac{\pi}{2aD}\right)^{1/2} \quad (9b)$$

is the surface concentration. The value of χ_0 is prescribed by Henry's law. The magnitude of the surface flux then follows from the last expression. The result shows that the concentration changes from its surface value to the value prevailing in the body of the fluid within a depth of the order of $(2D/a)^{1/2}$. For small diffusivity and large divergence, this concentration boundary layer can become very thin.

The mass transfer coefficient (velocity) is by definition $k = -F_0/\chi_0$; from (9b) this is found to be

$$k = (2aD/\pi)^{1/2} \quad (10a)$$

The solution at this stage applies to the z axis, which coincides with the $\psi = 0$ streamline. However, χ given by (9a) also satisfies the full differential equation (3), so that it is an exact solution at any x , given the flow field assumed. This verifies that horizontal diffusion may be neglected in the stagnation point region. In reality, of course, the horizontal extension of the divergent surface flow region is limited, and horizontal gradients must appear somewhere. What the results demonstrate is that under a line of surface divergence the diffusion boundary layer thickness is controlled by the divergence. Referring back to Fortescue and Pearson's model, one notes that the long plateau of the χ contours in the region of the surface divergence conforms to the stagnation point solution.

For later convenience, the usual nondimensional form of the mass transfer coefficient may also be written down here. Dividing by the friction velocity u^* ($=(\tau/\rho)^{1/2}$, where τ is wind stress and ρ is water density), one finds for $k^+ = k/u^*$

$$k^+ = 0.80 Pe^{-1/2} \quad (10b)$$

where the Peclet number is

$$Pe = u^{*2}/aD$$

The peak divergence in the Fortescue and Pearson model was $\pi u/L$, so that the result in (1) is almost identical with (10a), the constant in the former being somewhat larger. Because the numerically calculated constant in (1) applies to the average mass transfer over the cell, it is somewhat

surprising that it should be larger than the stagnation point result.

4. COMPARISON WITH THE SMOOTH SOLID SURFACE

It is instructive to repeat the above calculations for the case of a solid surface, over which a viscous boundary layer develops. The flow field around a stagnation point in that case is known as "Hiemenz flow" [Schlichting, 1960, p. 78]. Because the horizontal velocity has to vanish at the solid surface, so does $\partial u/\partial x$ and therefore by continuity $\partial w/\partial z$. Outside a thin boundary layer, however, the velocity components are as in the case of the free surface just discussed. Within the boundary layer the velocity and length scales are $(\nu a)^{1/2}$ and $(\nu/a)^{1/2}$, respectively, where a is the divergence outside the boundary layer and ν is viscosity. Schlichting gives the vertical velocity component as

$$w = (\nu a)^{1/2} \phi(\eta) \quad (11)$$

where $\phi(\eta)$ is a tabulated function of $\eta = -z(a/\nu)^{1/2}$ increasing at first quadratically with η , then approaching a linear asymptote.

The advection-diffusion problem is the same as before, except that w is now a more complicated function. The flux is found by the integration of the equivalent of (6):

$$\ln(F_0/F) = Sc \int_0^\eta \phi(\eta) d\eta \quad (12)$$

where $Sc = \nu/D$ is the Schmidt number. A second integration yields the concentration distribution

$$\chi_0 - \chi(z) = -(F_0/D) \cdot (\nu/a)^{1/2} \int_0^\eta \exp\left\{-Sc \int_0^\eta \phi(\eta) d\eta\right\} d\eta \quad (13)$$

Putting again $\chi(\infty) = 0$ and defining the mass transfer coefficient as before, one has

$$k = -F_0/\chi_0 = \frac{D(a/\nu)^{1/2}}{\varphi(Sc)} \quad (14)$$

where

$$\varphi(Sc) = \int_0^\infty \exp\left\{-Sc \int_0^\eta \phi(\eta) d\eta\right\} d\eta \quad (15)$$

giving a somewhat more complex relationship, which includes viscosity as well as diffusivity.

For the case of large Schmidt number, the quantity defined in (15) may be evaluated explicitly. The expansion of the profile $\phi(\eta)$ starts with

$$\phi(\eta) = \frac{c_2}{2} \eta^2 - \frac{1}{6} \eta^3 \dots \quad (16)$$

Schlichting gives the value of the second derivative, c_2 , as 1.2326. The first term in the expansion is accurate enough as long as $\eta \ll 3c_2 = 3.7$, say, up to $\eta = 0.4$. Integration of ϕ to this value of η yields about 0.13, so that the argument of the exponential in the integrand in (15), for Schmidt number of the order of 100 or higher, is already large compared with

unity. The integrand is then vanishingly small for this value of η and higher. With the upper limit taken to be infinity the integral can be evaluated explicitly, with the following result:

$$k = \beta Sc^{-2/3}(\nu a)^{1/2} \quad (17)$$

where

$$\beta = \frac{3(c_2/6)^{1/3}}{\Gamma(1/3)} = 0.66 \quad (18)$$

The nondimensional version of (17) is then

$$k^+ = 0.66 Sc^{-2/3} Re^{-1/2} \quad (19)$$

where the Reynolds numbers if $Re = u^{*2}/\nu$. For comparison, (10) may be rewritten as:

$$k^+ = 0.623 Sc^{-1/2} Re^{-1/2} \quad (20)$$

The two formulae are almost identical, the only significant difference being in the power of the Schmidt number. Note, however, that the formulation according to (20) is artificial: there is no viscosity dependence in (10). As *Deacon* [1981] points out, the $Sc^{-2/3}$ dependence has been well established by laboratory measurements in flow over solid surfaces. Surface renewal models have, on the other hand, suggested a $Sc^{-1/2}$ relationship, and this has been the accepted method of converting data on heat and mass transfer across gas-liquid interfaces taken at different Prandtl and Schmidt numbers [*Jähne et al.*, 1985]. The surface divergence models for a free and a solid surface clearly show how the difference arises.

5. THE ROLE OF BREAKING WAVELETS

As already mentioned, several studies have demonstrated that wind waves in laboratory flumes decisively influence free surface gas exchange [*Broecker et al.*, 1978; *Jähne et al.*, 1985, 1987]. Furthermore, *Jähne et al.* [1987] also showed that it was not the capillary waves that were involved. Earlier, *Deacon* [1981], upon careful analysis, concluded that the convergences and divergences associated with wave orbital velocities are too weak to affect gas transfer to a significant extent. This points then to the vortical motions involved in wave breaking as the likely conduits of DBL fluid downward. In breaking short waves the surface divergences are likely to be especially intense.

Toba and his collaborators have shown [*Toba*, 1985; *Ebuchi et al.*, 1987] that short wind waves generated in the laboratory carry accumulations of vortical fluid near the crest, collected in the steeper wavelets into a separation bubble or "roller." In a wave-following frame, the roller lies above a stagnation streamline surface, which intersects the free surface at the loci of convergence and divergence. Elsewhere (C. T. Csanady, Momentum flux in breaking wavelets, submitted to *Journal of Geophysical Research*, 1989, hereinafter referred to as Csanady (1989)) I have discussed the physical properties of these rollers and their role in air-sea momentum transfer. Of interest to gas transfer are the intensity of the divergence and the dimensions of the rollers.

Okuda's [1982] observations provided direct evidence on the intensity of the surface divergence in the steeper wave-

lets, the breaking of which was induced by the shear stress of the wind (*Okuda's* classes II and III; see Table 1 of *Csanady* (1990)). In a wave-following frame, the surface velocity changed from about 40 cm s⁻¹ in one direction to 10 cm s⁻¹ in the other within about 2 cm distance, an average divergence of 25 s⁻¹. This occurred at a friction velocity of about $u^* = 1$ cm s⁻¹, on wavelets of about 12 cm wavelength, and at celerity near 50 cm s⁻¹. The peak divergence due to wave motion was only about 8 s⁻¹; wave divergence was much less near the crest where the stagnation points were located. Therefore the most intense divergences were certainly associated with the rollers on breaking wavelets. The depth of the vortical fluid at wave crests was of the order of a millimeter, its vorticity of order $u^{*2}/\nu = 100$ s⁻¹.

In a first approximation the roller may be envisaged as a two-dimensional flow structure. Its intense internal vorticity originates from the viscous boundary layer on the upwind side of a wavelet, where a shear-stress spike is exerted by the wind. The surface vorticity in this region is $\gamma u^*/\nu$, where u^{*2} is the average kinematic wind stress and γ is an amplification factor empirically found to be about 6 [*Okuda*, 1982]. The vorticity within the roller was not much less, as was already mentioned (the peak vorticity could not be directly observed). If the volume of vortical fluid per spanwise length (the cross-sectional area of the roller) is b^2 , the circulation around the roller is of the order of $\Gamma = \gamma b^2 u^{*2}/\nu$. Velocities induced by the vorticity of the roller are then proportional to Γ/b , and the divergence is proportional to Γ/b^2 , i.e., to the vorticity again. Substitution into (10) now yields for the nondimensional mass transfer coefficient at a line of divergence

$$k^+ = \alpha Sc^{-1/2} \quad (21)$$

where α is a constant. The "pure" Schmidt number dependence of the nondimensional mass transfer coefficient in (21) arises from the postulate that the vorticity in the roller is inversely proportional to the viscosity. This should be true if the rollers, or more precisely the divergences they give rise to, occur on account of viscous stress variations at the surface.

Suppose now that the divergences on breaking wavelets provide the principal conduit for gas transfer. Because only a fraction of the surface can be covered by divergences, the average mass transfer coefficient will be less than the last result:

$$k^+ = \alpha \epsilon Sc^{-1/2} \quad (22)$$

where ϵ is the fraction of the surface effective in gas transfer, that fraction actually covered by divergences and the surrounding areas, where the DBL is comparably thin. The effective fraction ϵ is likely to change with wind speed, as short wavelets are raised, steepen, and perhaps saturate the surface. To sum up the physics underlying (22), the most intense divergences control gas transfer rate, and the intensity of those comes from variations of viscous stress exerted by the wind.

6. ROLLER MODEL

To estimate the magnitude of the constant α in (21), a crude model of the roller will be constructed by supposing the vorticity concentrated into a line vortex of circulation Γ

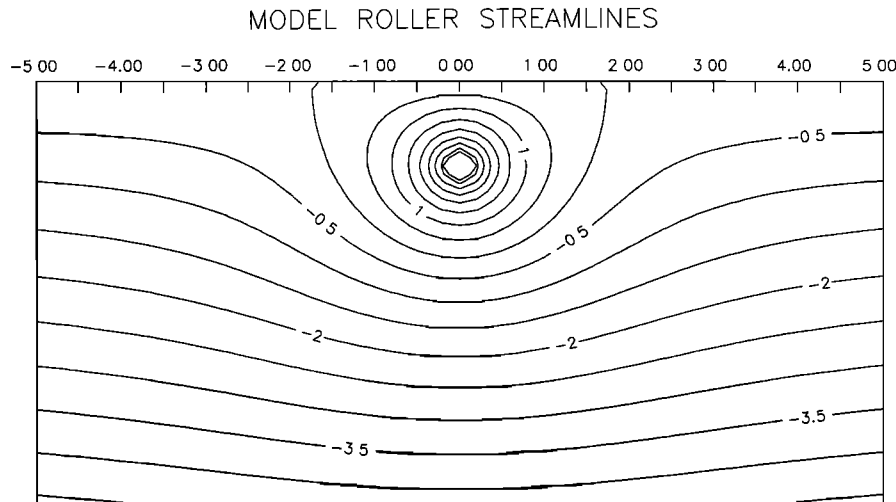


Fig. 1. Streamlines in and around two-dimensional roller model, generated by a line vortex placed a unit distance below the surface, in a stream of unit velocity. The vortex is made stationary by choosing its circulation to be 4π . Leading and trailing stagnation points are at $x = \pm 3^{1/2}$, where the convergence or divergence is $3^{1/2}/2$. Stream function contours are in unit distance times unit velocity; the zero contour outlines the roller.

at a distance b below the surface. A far-field velocity has to be added to make the vortex stationary. The streamline field of such a vortex is, in a vortex-following frame [Lamb, 1957],

$$\psi = \frac{\Gamma}{2\pi} \left(\frac{z}{2b} - \ln \frac{r_1}{r_2} \right) \quad (23)$$

where r_1 and r_2 are radii from the vortex and its image above the surface. After some elementary calculations, one finds for the approach velocity far from the vortex, U , and the surface divergence at the divergence line, a ,

$$U = \frac{\Gamma}{4\pi b} \quad (24)$$

$$a = \frac{3^{1/2}\Gamma}{8\pi b^2} = \frac{3^{1/2}U}{2\pi b} \quad (25)$$

Figure 1 illustrates the streamlines given by (23), with distances made nondimensional using the scale b , the stream function by Ub .

The average vorticity in the roller is circulation divided by area, or about $0.55 \Gamma/b^2$. The divergence a is therefore only about 13% of the originating vorticity. In Okuda's case II and III waves, the peak vorticity was $\gamma u^{*2}/\nu = 600 \text{ s}^{-1}$, the average vorticity in the roller of order 100 s^{-1} . The observed divergence of 25 s^{-1} was thus also much less than the vorticity. If crude, the roller model gives the right order of magnitude for the divergence.

Using (25), the constant α in (22) turns out to be

$$\alpha = \frac{u^*}{2\pi} 3^{1/4} \gamma^{1/2} = 0.513 \quad (26)$$

Jähne *et al.* [1987], in their thorough essay on the mass transfer coefficient, have emphasized that the inverse square root dependence on Schmidt number remains valid when viscosity and diffusivity are varied independently. In other words, there is no separate Reynolds number influence, and

(22) covers all the molecular effects. This has been deduced here by attributing the divergence to viscous stress variations.

Extrapolated back to a Schmidt number of unity, Jähne *et al.* found $k^+ = 0.1$, at a friction velocity of $u^* = 0.01 \text{ m s}^{-1}$. The effective surface fraction ε in (22) would have to be about 0.2 to simulate this result. At higher friction velocity the fraction would have to be higher still. The comparison with observation thus suggests that a relatively large fraction of the surface carries divergences, or more precisely that the DBL is not much thicker than over the divergences, over a large fraction of the surface. This is somewhat surprising and calls for a detailed investigation of the flux distribution near a roller.

7. DIFFUSION IN THE ROLLER

To explore the interplay of advection and diffusion in and around the roller, the high Peclet number of the problem is advantageously exploited. The circulation around the roller, Γ is measured in tens of square centimeters per second, while the diffusivity D is typically a million times smaller. The ratio of the length scale of the roller, b , to the boundary layer thickness over the divergence, $\delta = (2D/a)^{1/2}$, is then

$$\sigma \equiv b/\delta = \left(\frac{3^{1/2}}{16\pi} Pe \right)^{1/2} \quad (27)$$

which has a typical value of 300. Here $Pe = \Gamma/D$ is a Peclet number, and the value of a has been substituted from (25). When interest centers on a surface layer only a few times deeper than δ , it is legitimate to neglect the small change of velocity with depth. The near-surface advection field will therefore be described by

$$u = u(x) = U \left(1 - \frac{4b^2}{b^2 + x^2} \right) \quad (28a)$$

$$w = -z \frac{du}{dx} \quad (28b)$$

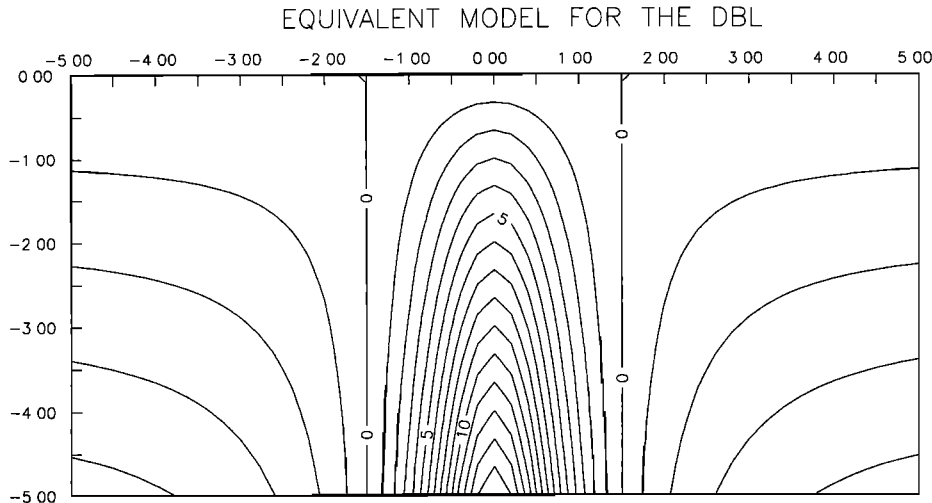


Fig. 2. Streamlines in a model with horizontal velocity constant with depth, equal to the surface velocity in the previous model. Horizontal distances have been slightly squeezed to make roller width a rational number, 3 distance units instead of $2(3)^{1/2}$, with the roller extending from $x = -1.5$ to $x = 1.5$. In a very thin layer near the surface the two models are otherwise equivalent.

$$\psi = zu(x) \tag{28c}$$

The boundary condition remains as in the simpler problems discussed before: $\chi = \chi_0$ at the surface, vanishing χ at depth. At the line of divergence, $x = 3^{1/2} b$, earlier results suggest a smooth variation of the concentration with x , on the b scale, so that horizontal diffusion may be neglected:

$$\left| \frac{\partial^2 \chi}{\partial x^2} \right| \ll \left| \frac{\partial^2 \chi}{\partial z^2} \right| \tag{29}$$

This then leaves a parabolic equation to be solved:

$$u \frac{\partial \chi}{\partial x} = D \frac{\partial^2 \chi}{\partial z^2} + z \frac{du}{dx} \frac{\partial \chi}{\partial z} \tag{30}$$

Such an equation can be solved step by step in the direction of the velocity u , beginning at a line of divergence and ending at a convergence. The calculations are best carried out in terms of nondimensional variables, defined by the following assignments:

$$\begin{aligned} x &\Rightarrow ax/U & z &\Rightarrow z/\delta \\ u &\Rightarrow u/U & \psi &\Rightarrow \psi/U\delta \\ \chi &\Rightarrow \chi/\chi_0 & F &\Rightarrow F/a\delta\chi_0 \end{aligned}$$

where $\delta = (2D/a)^{1/2}$, the diffusion boundary layer thickness over the divergence, and $a = |du/dx|_a$ is the value of the divergence, at the line of divergence. In terms of these variables, (30) takes on the form

$$u \frac{\partial \chi}{\partial x} = \kappa \frac{\partial^2 \chi}{\partial z^2} + z \frac{du}{dx} \frac{\partial \chi}{\partial z} \tag{31}$$

where $\kappa = 1/2$ is a nondimensional diffusivity. The vertical diffusive flux is

$$F = -\kappa \frac{\partial \chi}{\partial z} \tag{32}$$

and the streamlines are described by

$$\psi = z - \frac{4z}{1 + 4x^2/3} \equiv zu(x) \tag{33}$$

a result easily reconciled with (23) by expanding the logarithm near $z = 0$. Owing to the different choice of horizontal scale, the line of divergence is now located at $x = 3/2$, instead of $3^{1/2}$, as in Figure 1. Figure 2 shows the streamline field according to (33). While at depths of the order of 1 (dimensional b) the flow pattern differs greatly from the roller model of Figure 2, it is the same at depths of order δ , which is all that counts. The point these figures demonstrate is that the details of the eddy flow pattern at depth are irrelevant, only the convergence and divergence matters.

At the line of divergence, the horizontal velocity vanishes, and (31) becomes an ordinary differential equation for which a solution is easily obtained and the boundary conditions satisfied, as has already been demonstrated. In the neighborhood of this line one may expand the solution $\chi(x, z)$ and the velocity $u(x)$ in terms of the distance $\xi = x - 3/2$ as follows:

$$\chi = c_0(z) + c_1(z)\xi + \dots \tag{34a}$$

$$u = \xi - \frac{2}{3}\xi^2 + \dots \tag{34b}$$

Substituting into (31), and collecting the zero- and first-order terms separately, one finds the two equations

$$c_0'' + 2zc_0' = 0 \tag{35a}$$

$$c_1'' + 2zc_1' - 2c_1 = 2zc_0' \tag{35b}$$

where primes denote differentiation with respect to z . For boundary conditions, one must prescribe $c_0 = 1, c_1 = 0$ at the surface and both vanishing at great depth. The solutions may be found by standard methods and are:

$$c_0 = \text{erfc}(-z) \tag{36a}$$

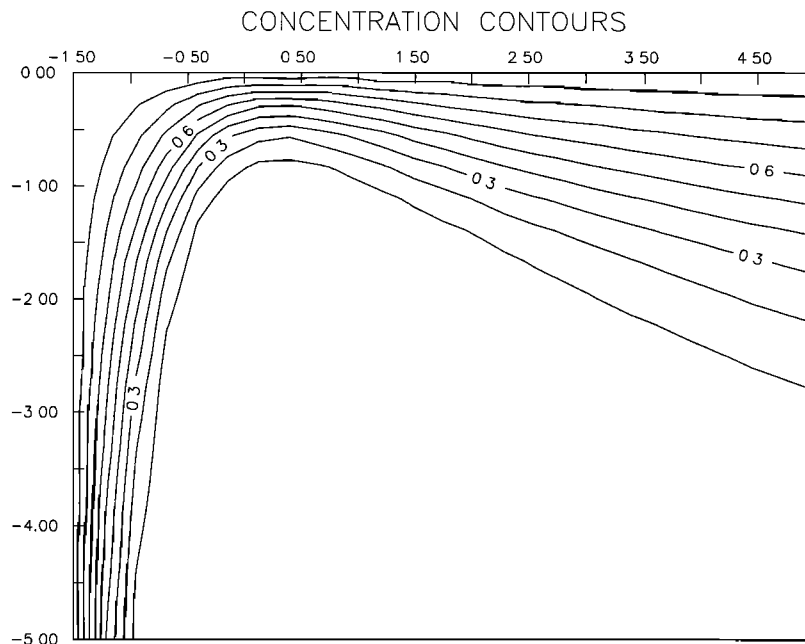


Fig. 3. Contours of constant concentration in the roller and downstream, scaled by the concentration difference across the DBL. Horizontal distances are the same as in the previous figure, but the vertical coordinate has been stretched; the depth unit is now the DBL thickness under the divergence line at $x = 1.5$. The contours cross the divergence line smoothly, but under the convergence line there is a singularity where a downwelling plume carries surface fluid into the interior.

$$c_1 = \frac{\pi^{1/2}}{6} z \exp(-z^2) \tag{36b}$$

$$\chi = \operatorname{erfc} \left(\frac{\psi}{2(\kappa\tau)^{1/2}} \right) \equiv \operatorname{erfc} \left(\frac{z}{\zeta} \right) \tag{41}$$

the first one being the nondimensional version of (9).

Given this start, one could now calculate a solution to (31) numerically. A more efficient method is, however, available, based on the von Mises transformation [Schlichting, 1960, p. 136]. Where the velocity u is nonzero, the vertical coordinate z may be replaced by the stream function ψ . The advection-diffusion equation (31) transformed to x, ψ coordinates is (see, for example, Levich [1962, p. 79]):

$$\frac{\partial \chi}{\partial x} = \kappa \frac{\partial}{\partial \psi} \left(u \frac{\partial \chi}{\partial \psi} \right) \tag{37}$$

The surface is understood to be the $\psi = 0$ streamline, and the boundary condition $\chi = \chi_0$ is prescribed here. Because u is a function of x alone, it may be absorbed in the horizontal variable as follows:

$$\tau = \int_{3/2}^{\xi} u \, dx \tag{38}$$

which results in

$$\frac{\partial \chi}{\partial \tau} = \kappa \frac{\partial^2 \chi}{\partial z^2} \tag{39}$$

For this simple form of the heat conduction equation it is necessary to prescribe initial conditions, in addition to the boundary conditions already mentioned. In the present case,

$$\chi(\xi = 0, z) = c_0(z) \tag{40}$$

One solution of (39) satisfying the boundary conditions is

where $\zeta = 2(\kappa\tau)^{1/2}/u$ is a local depth scale, $\psi = zu(x)$ having been substituted in the second equality. The presence of the velocity in the denominator of ζ may seem odd; it comes about because diffusion time t varies as x/u , while τ is ux , or u^2t . The square root of this cancels u in the denominator and leaves $\zeta \sim (\kappa t)^{1/2}$, as one expects.

Both u and τ tend to zero at $\xi = 0$. Putting $u = |du/dx|_0 \xi$ near the line of divergence, using the definition of τ in (38) and noting that $\kappa = 1/2$, one finds that $\zeta \Rightarrow 1$ at $\xi = 0$. This result is independent of the specific form of the surface velocity distribution away from the line of divergence. A value of $\zeta = 1$ means that the solution c_0 of (36a) is recovered. Remarkably enough, then, the solution written down in (41) satisfies the initial condition, (40), and so constitutes an exact solution of the advection-diffusion problem posed, for arbitrary $u(x)$.

For the specific choice of the velocity in the roller model, integration of $u(x)$ yields the distance variable τ in closed form:

$$\tau = x - \frac{3}{2} + 2(3^{1/2}) \left[\frac{\pi}{3} - \tan^{-1} \left(\frac{2x}{3^{1/2}} \right) \right] \tag{42}$$

With the aid of this expression, the concentration field of the roller model may be calculated on both sides of the divergence line. At large positive x , one finds $\tau = x - 3/2 - \pi/3^{1/2}$. Over the roller itself, τ rises monotonically to $\tau = 4\pi/3^{1/2} - 3 = 4.26$ at the convergence line, $x = -3/2$. At still greater negative x the advection-diffusion problem cannot be solved without specifying some entry profile for the concen-

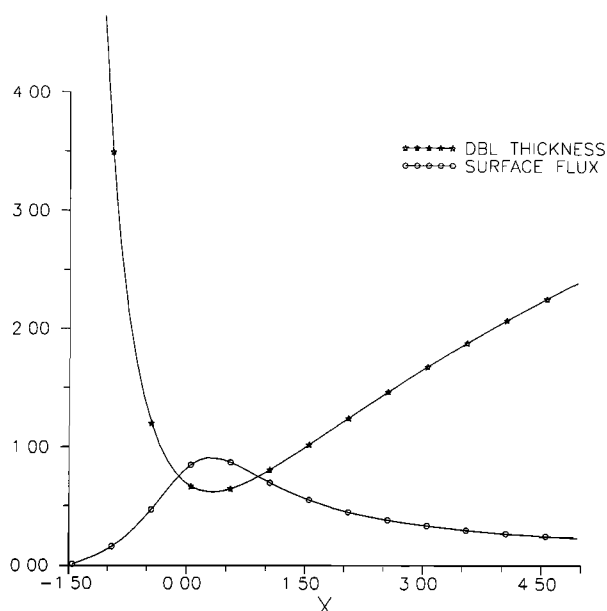


Fig. 4. Surface flux F_s and DBL thickness ζ over the roller and downstream. Under the convergence line at $x = -1.5$, ζ is singular, tending to infinity, while the flux vanishes, being proportional to ζ^{-1} . Minimum ζ and maximum flux occur on the divergent side of roller center; here the flux is considerably higher than over the divergence line at $x = 1.5$ (where it is $F_s = 1/\pi^{1/2}$).

tration. Figure 3 shows the concentration field for $x > -3/2$. The scale of nondimensional z is the same as of nondimensional x , but this of course amounts to a stretching of the z coordinate in the ratio $U/a\delta$. The descending plume and the slow growth of the DBL in the direction of positive x are clear.

Figure 3 illustrates the fallacy of regarding eddy flux independent of molecular diffusion in the vicinity of the free surface. Consider conditions at $z = -3\delta$, for example. The horizontally averaged concentration gradient, $\partial\chi/\partial z$, is vanishingly small, the flux is essentially the same as at the surface, $F = F_0$. The eddy diffusivity is then much larger than molecular diffusivity, as in the well mixed fluid below. For gas diffusion, this occurs at a depth of some $30 \mu\text{m}$. For heat diffusion in the same eddy field at the same depth, the flux is mostly molecular, and the eddy flux and eddy diffusivity are small. Thus neither eddy flux nor eddy diffusivity is a property of the eddies alone.

8. FLUX LINES

The most important predictions of the roller model concern the flux of the substance exchanged at the surface, and how this flux is disposed of within the body of the fluid. From the solution in (41) one finds at once for the vertical diffusive flux:

$$F = -\frac{2\kappa}{\pi^{1/2}\zeta} \exp\left(-\frac{z^2}{\zeta^2}\right) \quad (43)$$

The surface value of this, $F_s = 2\kappa/(\pi^{1/2}\zeta)$, is the flux entering the fluid, which is seen to vary as ζ^{-1} . Figure 4 illustrates the variation of the diffusion boundary layer depth ζ and of F_s . On the downstream side, ζ increases, and F_s decreases monotonically and fairly sluggishly on the b scale.

Over the roller the boundary layer depth at first decreases toward negative x , (surprisingly perhaps) bottoms out, and becomes very large at the convergence line. The surface flux mirrors this behavior.

In interpreting the solution near the convergence line one must remember that it describes molecular diffusion and advection by a specific eddy, at depths on the δ scale. Where the boundary layer depth grows large on this scale, the flow and the concentration field merge into the well-mixed turbulent interior. On the vertical streamline $\psi = 0$ under the convergence, (41) shows the concentration to equal its surface value, $\chi = 1$ (dimensional χ_0). Here a plume of boundary layer fluid is descending into the interior, to be mixed by eddies at depths on the b scale.

The fate of the boundary layer fluid is exhibited particularly clearly by "flux lines," analogous to streamlines, of the total flux vector (molecular plus advective flux). The diffusion equation states that the total flux is nondivergent, so that it can be described by a flux function $\phi(x, z)$, analogous to a stream function, the derivatives of which equal the components of the total flux:

$$\frac{\partial\phi}{\partial z} = u\chi \quad \frac{\partial\phi}{\partial x} = -w\chi + \kappa \frac{\partial\chi}{\partial z} \quad (44)$$

Integrating the first of these equations, with (41) substituted for χ , one finds at once

$$\phi = u\zeta \operatorname{ierfc}\left(-\frac{z}{\zeta}\right) = \pm 2(\kappa\tau)^{1/2} \operatorname{ierfc}\left(-\frac{z}{\zeta}\right) \quad (45)$$

the flux function being negative over the roller, positive downstream. Figure 5 illustrates the pattern of flux lines. Under the convergence line the flux function has a value of $-2(\kappa\tau/\pi)^{1/2}$, which equals -1.65 in the present case. The average flux over the roller, three nondimensional units long, is thus -0.55 , almost the same as the flux over the divergence line, $-1/\pi^{1/2} = -0.56$.

As already remarked, the solution written down in (41) is valid for any $u(x)$, so that the qualitative features of the concentration and flux fields remain very similar if other eddy models are used, as long as the eddy scale remains large compared with the DBL scale. Fortescue and Pearson's model, for example, is described in terms of the present scaling by

$$u = \sin(x) \quad (46)$$

This yields $\tau = 1 - \cos(x)$, which grows from zero to 2 between the divergence and the convergence. The flux function correspondingly varies at the surface between zero and $2 \operatorname{ierfc}(0) = 1.1284$. This is the value of the constant given by the exact solution for (1), replacing Fortescue and Pearson's 1.46 obtained by numerical integration.

9. CONCLUDING REMARKS

A case has been made above for the proposition that the most intense surface divergences, responsible for what was called in the early literature surface renewal, are caused on a wind-blown surface by viscous surface stress variations associated with breaking wavelets. Gas transfer is controlled by these divergences as they keep the diffusion boundary layer thin. The combination of two very simple ideas,

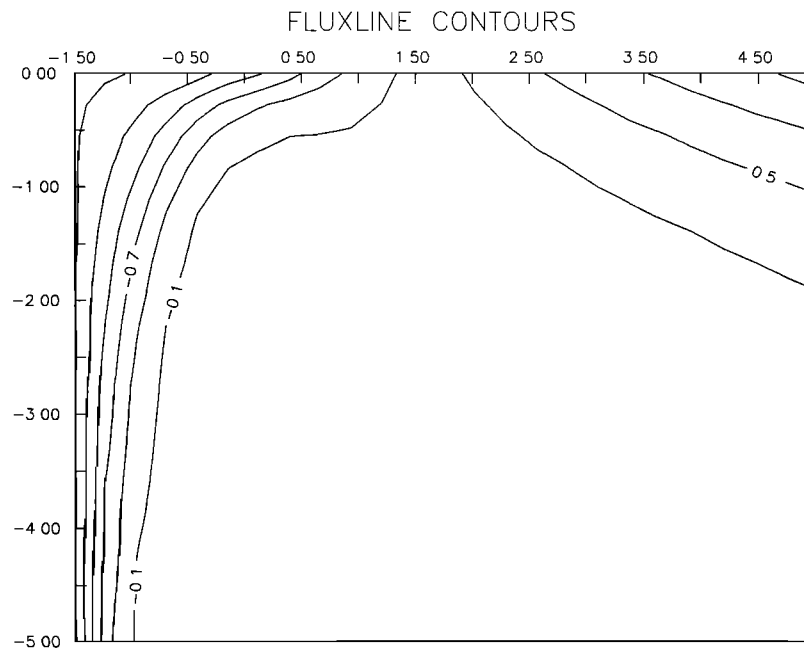


Fig. 5. Flux lines (lines parallel to the total flux vector, analogous to streamlines) in the roller and downstream. The flux lines within the roller are all collected by the downwelling plume, while the flux lines originating beyond the roller follow the divergent flow downstream. Units are the concentration difference across the DBL times the velocity scale; the flux in these units integrated over the roller is 1.65. The minimum flux line contour, coinciding with the vertical line under the convergence, has thus the label -1.65 .

interaction of diffusion with advection in divergent stagnation point flow, and shear layer-fluid accumulation on a breaking wavelet, allowed the construction of an eddy-resolving analytical model of gas transfer. The results were in qualitative and quantitative agreement with laboratory observations. One parameter is left free by the model, expressing the fraction of the surface covered by divergences, or rather by a DBL not much thicker than one finds over the divergences. A detailed examination of the diffusion and flux fields also showed that the DBL remains thin and that the flux remains high over a moderately broad region around the rollers.

Clearly, the free parameter ϵ , gauging the fraction of the surface effective in gas transfer, is a likely cause of differences between laboratory and open ocean. While with increasing wind speed the surface coverage of divergences should saturate and stay constant in the laboratory, orbital motions of large waves may suppress the short wavelets in wave troughs and reduce ϵ . When large waves break, they have been shown to eliminate small wavelets altogether near the large wave crest [Banner *et al.* 1989]. This should reduce ϵ , but of course bubbles and spray produced in breaking waves would tend to increase gas transfer, and the net effect of large wave breaking on k is uncertain.

If ϵ did drop with wind speed on account of the effects just mentioned, the increase of k with u^* would be reduced or eliminated. This might be a partial explanation of low transfer rates observed in the open ocean. At any rate, the gross variations of wave climate over the open ocean should result in major changes in ϵ , a possible reason for the large scatter of field gas transfer data as a function of u^* . Perhaps the radar signature of the wave surface, in a band tuned to the short wavelets, would be a better predictor of gas transfer than u^* alone. Recent work by Banner and Fooks

[1985] indeed suggests that the radar return in the 4-cm wave band is mainly due to surface perturbations on rollers. In view of the possibility of global monitoring, the connection between gas transfer and radar return would certainly be worth exploring in detail.

Acknowledgments. The work described herein was supported by the Office of Naval Research, under a contract entitled "Wavelets and Turbulence over the Sea Surface."

REFERENCES

- Banner, M. L., and E. H. Fooks, On the microwave reflectivity of small-scale breaking water waves, *Proc. R. Soc. London, Ser. A*, 399, 93–109, 1985.
- Banner, M. L., I. S. F. Jones, and J. C. Trinder, Wavenumber spectra of short gravity waves, *J. Fluid Mech.*, 198, 321–344, 1989.
- Bolin, B., On the exchange of carbon dioxide between atmosphere and sea, *Tellus*, 12, 274–281, 1960.
- Broecker, H. C., J. Petermann, and W. Siems, The influence of wind on CO_2 exchange in a wind-wave tunnel, including the effect of monolayers, *J. Mar. Res.*, 36, 595–610, 1978.
- Broecker, W. S., and T. H. Peng, Gas exchange rates between air and sea, *Tellus*, 26, 21–35, 1974.
- Brtko, W. J., and R. L. Kabel, Transfer of gases at natural air-water interfaces, *J. Phys. Oceanogr.*, 8, 543–556, 1978.
- Coantic, M., A model of gas transfer across air-water interfaces with capillary waves, *J. Geophys. Res.*, 91, 3925–3943, 1986.
- Danckwerts, P. V., Significance of liquid-film coefficients in gas absorption, *Ind. Eng. Chem.*, 43, 1460–1467, 1951.
- Deacon, E. L., Gas transfer to and across an air-water interface, *Tellus*, 29, 363–374, 1977.
- Deacon, E. L., Sea-air gas transfer: The wind speed dependence, *Boundary Layer Meteorol.*, 21, 31–37, 1981.
- Ebuchi, N., H. Kawamura, and Y. Toba, Fine structure of laboratory wind-wave surfaces studied using an optical method, *Boundary Layer Meteorol.*, 39, 133–151, 1987.

- Fortescue, G. E., and J. R. A. Pearson, On gas absorption into a turbulent liquid, *Chem. Eng. Sci.*, 22, 1163-1176, 1967.
- Hasse, L., and P. S. Liss, Gas exchange across the air-sea interface, *Tellus*, 32, 470-481, 1980.
- Higbie, R., The rate of absorption of a pure gas into a still liquid during short periods of exposure, *Trans. Am. Inst. Chem. Eng.*, 31, 365-388, 1935.
- Jähne, B., T. Wais, L. Memery, G. Gaulliez, L. Merlivat, K. O. Münnich, and M. Coantic, He and Rn gas exchange experiments in the large wind-wave facility of IMST, *J. Geophys. Res.*, 90, 11,989-11,998, 1985.
- Jähne, B., K. O. Münnich, R. Börsinger, A. Dutzi, W. Huber, and P. Libner, On the parameters influencing air-water gas exchange, *J. Geophys. Res.*, 92, 1937-1949, 1987.
- Lamb, H., *Hydrodynamics*, 738 pp., Cambridge University Press, New York, 1957.
- Lamont, J. C., and D. S. Scott, An eddy cell model of mass transfer into the surface of a turbulent liquid, *AIChE J.*, 16, 513-519, 1970.
- Ledwell, J. J., The variation of the gas transfer coefficient with molecular diffusivity, in *Gas Transfer at Water Surfaces*, edited by W. Brutsaert and G. H. Jirka, pp. 293-302, D. Reidel, Hingham, Mass., 1984.
- Levich, V. G., *Physicochemical Hydrodynamics*, 700 pp., Prentice Hall, Englewood Cliffs, N. J., 1962.
- Okuda, K., Internal flow structure of short wind waves, I, On the internal vorticity structure, *J. Oceanogr. Soc. Jpn.*, 38, 28-42, 1982.
- Peng, T. H., W. S. Broecker, G. G. Mathieu, Y. H. Li, and A. E. Bainbridge, Radon evasion rates in the Atlantic and Pacific oceans as determined during the GEOSECS program, *J. Geophys. Res.*, 84, 2471-2486, 1979.
- Schlichting, H., *Boundary Layer Theory*, 647 pp., McGraw Hill, New York, 1960.
- Toba, Y., Wind waves and turbulence, in *Recent Studies in Turbulent Phenomena*, edited by T. Tsumi, H. Maruo, and H. Takami, pp. 277-296, Association of Scientific Document Information, Tokyo, 1985.

G. T. Csanady, College of Sciences, Department of Oceanography, Old Dominion University, Norfolk, VA 23529.

(Received April 12, 1989;
accepted June 9, 1989.)